SUPPORTING INFORMATION

Enhancing the Intrinsic Antiplasmodial Activity and Improving the Stability and Selectivity of a Tunable Peptide Scaffold Derived from Human Platelet Factor 4

Nicole Lawrence,[1*] Thomas N.G. Handley,[2,3] Simon J. de Veer,[1] Maxim D. Harding,[1] Alicja Andraszek,[1]

Lachlan Hall,[1] Karoline D. Raven,[4] Sandra Duffy,[5] Vicky M. Avery,[5] David J. Craik,[1] Lara R. Malins,[6] Brendan

J. McMorran.[4*]

[1] Institute for Molecular Bioscience and Australian Research Council Centre of Excellence for Innovations in Peptide and Protein Science, The University of Queensland, Brisbane, Queensland, 4072, Australia

[2] Department of Radiopharmaceutical Sciences, Cancer Imaging, The Peter MacCallum Cancer Centre, Victoria 3000, Australia

[3] Sir Peter MacCallum Department of Oncology, The University of Melbourne, Victoria, 3010, Australia

[4] The John Curtin School of Medical Research, College of Health and Medicine, Australian National University, Canberra, Australian Capital Territory, 2601, Australia

[5] Discovery Biology, Centre for Cellular Phenomics, School of Environment and Science, Griffith University, Nathan, Queensland, 4111, Australia

[6] Research School of Chemistry and Australian Research Council Centre of Excellence for Innovations in Peptide and Protein Science, Australian National University, Canberra, Australian Capital Territory, 2601, Australia

* Correspondence:

n.lawrence@imb.uq.edu.au

brendan.mcmorran@anu.edu.au

Table S1. Amino Acid Sequence and Mass of PDIP Analogues [a]

Set ID	Peptide	1 2 3 4 12345678901234567890123456789012345678901234567890	C-terminus	Exp mw [b]	Obs mw [c]
ref [1]	**1**	CGGPLYKKIIKKLLESGGSGGAPLYKKIIKKLCES*	amide	3718.6	3718.5
ref [2]	**2**	-GGPLYKKIIKKLLESGGSGGAPLYKKIIKKLC*	thioether, amide	3441.2	3440.9
ref [3]	**3**	**G**CGGPLYKKIIKKLLESGGSGGAPLYKKIIKKLCES*	amide	3775.6	3775.2
Set 1. substitute charged or hydrophobic residues	**4**	GCGGPLYKKIIKKLLESGGSGGAPLYKKIIKKLC*	ΔES, amide	3559.4	3558.8
	5	GCGGPLY**R**KIIKKLLESGGSGGAPLY**R**KIIKKLC*	ΔES, amide	3615.5	3614.8
	6	GCGGPLYK**R**IIKKLLESGGSGGAPLYK**R**IIKKLC*	ΔES, amide	3615.5	3614.8
	7	GCGGPLYKKII**R**KLLESGGSGGAPLYKKII**R**KLC*	ΔES, amide	3615.5	3614.8
	8	GCGGPLYKKIIK**R**LLESGGSGGAPLYKKIIK**R**LC*	ΔES, amide	3615.5	3614.8
	9	GCGGPLY**RR**II**RR**LLESGGSGGAPLY**RR**II**RR**LC*	ΔES, amide	3783.5	3783.3
	10	GCGGPLYKKIIKKLL**K**SGGSGGAPLYKKIIKKLC*	ΔES, amide	3588.5	3588.0
	11	GCGGPLYKKII**R**KLL**K**SGGSGGAPLYKKII**R**KLC*	ΔES, amide	3614.5	3614.1
	12	GCGGPLYKKIIKKLL**K**SGGSGGAPLYKKIIKKLCES*	amide	3774.6	3774.0
	13	GCGGPLYKKIIKKLL**K**SGGSGGAPLYKKIIKKLC**K**S*	amide	3773.7	3773.0
	14	GCGGPLYKKI**V**KKLLESGGSGGAPLYKKI**V**KKLC*	ΔES, amide	3531.4	3530.8
	15	GCGGPLYKKIIKK**H**LE**R**GGSGGAPLYKKIIKK**H**C*	ΔES, amide	3676.5	3676.0
	16	GCGGPL**W**KKIIKKLLESGGSGGAPL**W**KKIIKKLC*	ΔES, amide	3605.5	3605.1
Set 2. modify C-terminus	**17**	GCGGPLYKKIIKKLLESGGSGGAPLYKKIIKKLC	ΔES, carboxyl	3560.4	3559.6
	18	GCG**A**PLYKKIIKKLLESGGSGGAPLYKKIIKKLCES*	amide	3789.6	3789.3
	19	GCG**A**PLYKKIIKKLLESGGSGGAPLYKKIIKKLCES	carboxyl	3790.6	3790.4
	20	-GCG**A**PLYKKIIKKLLESGGSGGAPLYKKIIKKLCES-	backbone cyclic	3772.6	3772.0
	21	-GCG**A**PLYKKIIKKLLESGGSGGAPLYKKIIKKLCE**N**-	backbone cyclic	3799.6	3799.2
	22	-GCG**A**PLYKKIIKKLLESGGSGGAPLYKKIIKKLC**QN**-	backbone cyclic	3798.7	3798.4
	23	-GCG**A**PLYKKIIKKLLESGGSGGAPLYKKIIKKLC**KN**-	backbone cyclic	3798.7	3798.0
	24	-GG**A**PLYKKIIKKLLESGGSGGAPLYKKIIKKLLESGGS-	backbone cyclic	3882.7	3881.8
	25	-GG**A**PLYKKIIKKLLE**N**GGSGGAPLYKKIIKKLLE**N**GGS-	backbone cyclic	3936.7	3935.6
combined	**26**	-GG**A**PLYKKIIKKLL**K**SGGSGGAPLYKKIIKKLLESGGS-	backbone cyclic	3881.7	3881.1
	27	-GG**A**PLYKKIIK**R**LLESGGSGGAPLYKKIIK**R**LLESGGS-	backbone cyclic	3938.7	3938.0

[a] Peptides with Cys residues (shaded) contain a disulfide bond; C-terminal amide is shown as *; except peptide **2** (thioether macrocycle), peptides with C-terminal amide or carboxylic acid (carboxyl) are disulfide macrocycles; backbone cyclic peptides are indicated by – at N- and C-termini; changes to the amino acid sequence compared to peptide **3** are shown in bold

[b] Expected (exp) mass was calculated as the average mass from contributing amino acids

[c] Observed (obs) mass was determined from +4 m/z ions from mass spectrometry. Deviation of less than 0.03% of expected mass was observed for all peptides

Set 1: charge and hydrophobic substitutions

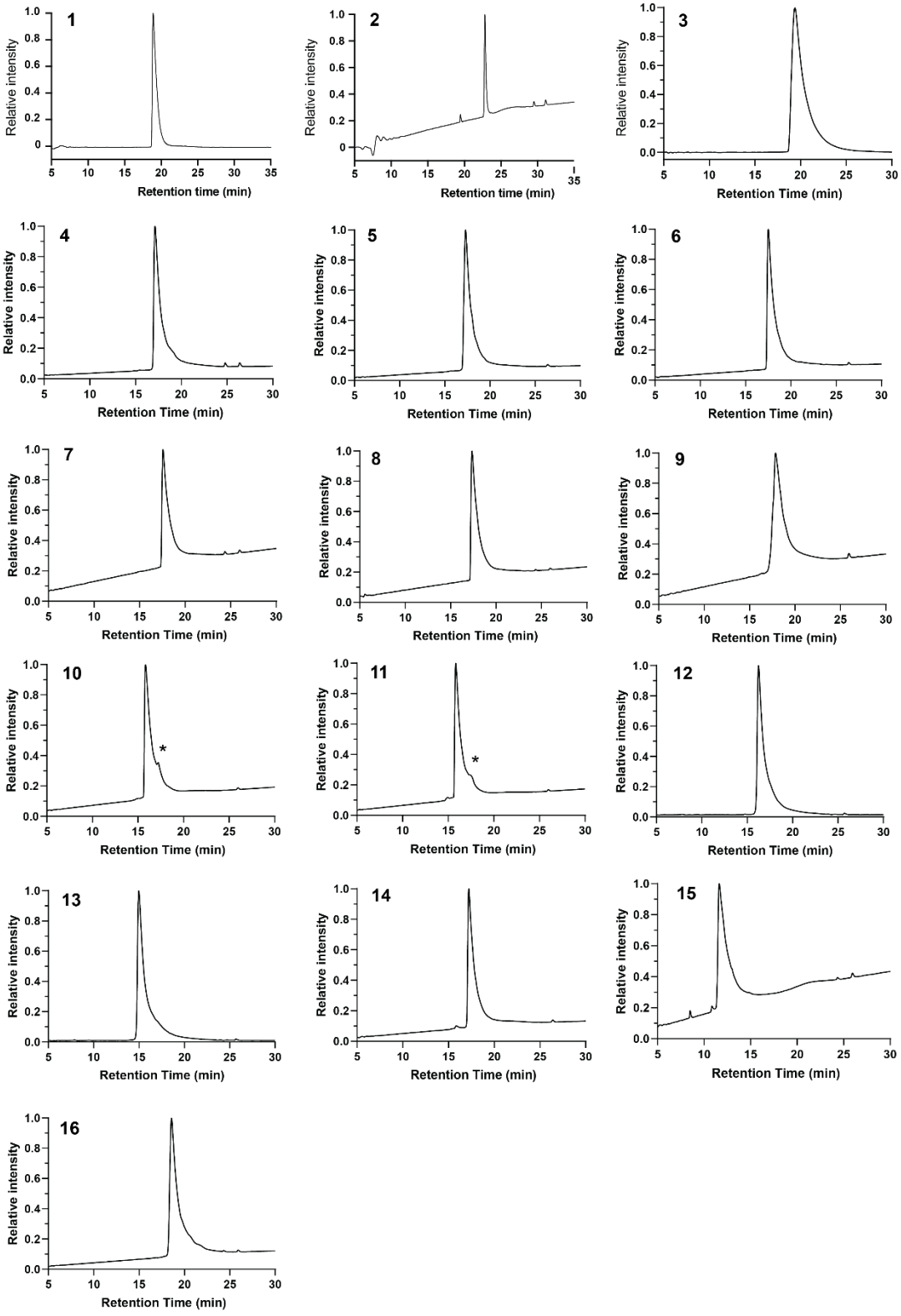

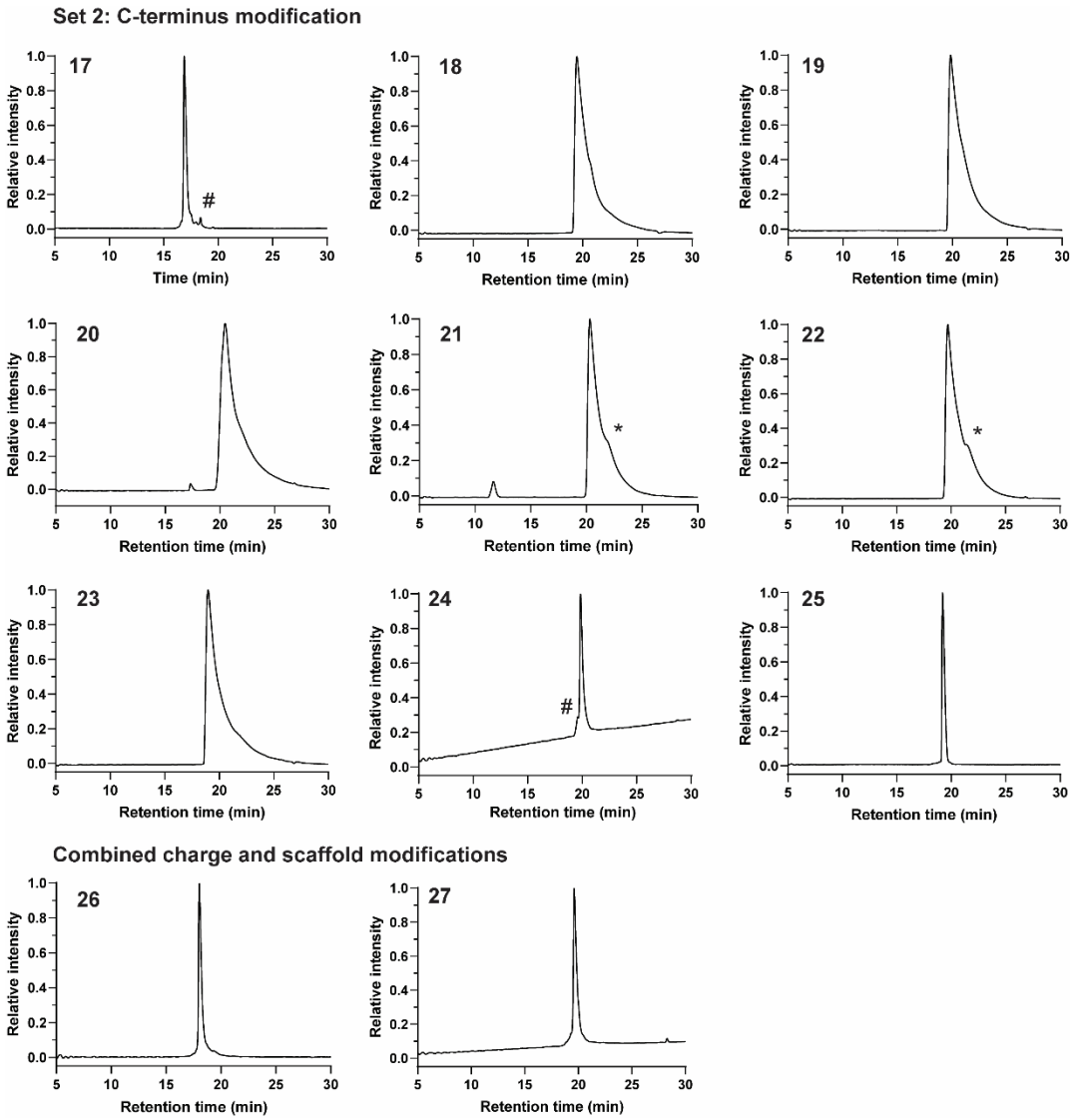

Figure S1. HPLC Trace of PDIP Analogues. Recorded using a Shimadzu LCMS-2020 instrument with a Phenomenex 5 µm C18 / 300 Å / 150 x 2 mm LC column. Peptides (~ 0.1 mg) were dissolved in solvent A (0.1% formic acid) and running a 2% B/min gradient (solvent B, 90% acetonitrile, 0.1% formic acid), starting from 1% solvent A. Spectra were recorded at 214 nm and are shown relative to the highest signal for each peptide. * indicates a shoulder peak with identical mass; # indicates a residual impurity of ≤5%.

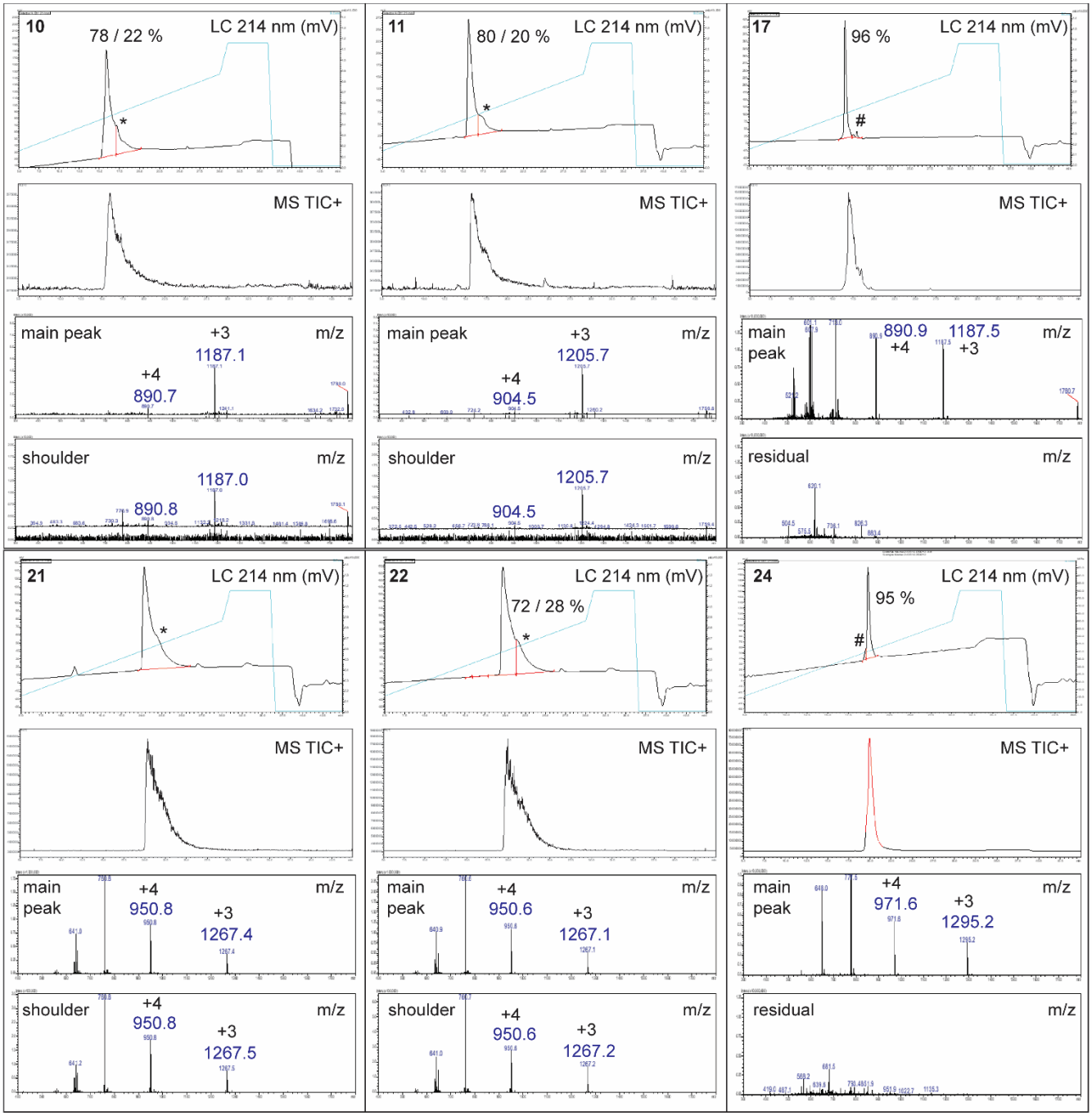

Figure S2. Integration and MS Characterization of PDIP Analogues from Analytical HPLC Trace. HPLC trace and MS data were simultaneously recorded using a Shimadzu LCMS-2020 instrument with a Phenomenex 5 µm C18 / 300 Å / 150 x 2 mm LC column. Analogues **10**, **11**, **21**, **22** have an apparent shoulder on the LC trace (indicated by * with relative proportions shown for the main peak/ shoulder) that was determined to have identical mass according to m/z peaks from the MS trace. Analogues **17** and **24** have residual impurity comprising ≤5% (indicated by #).

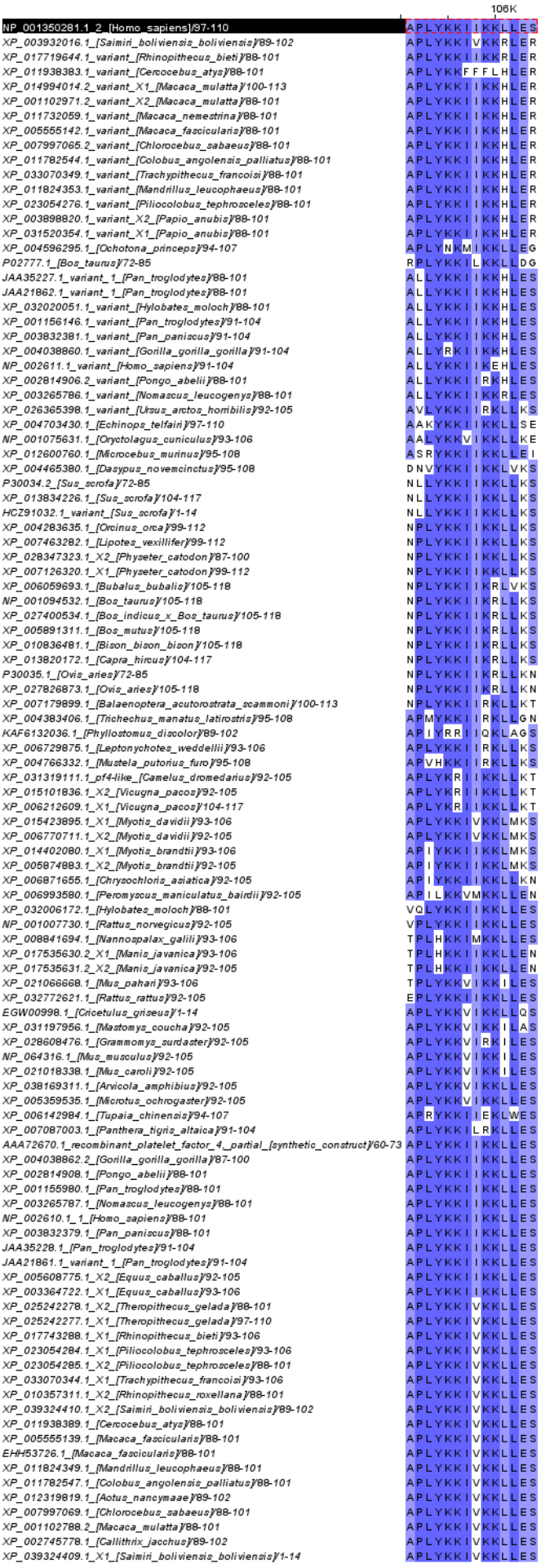

Figure S3. Alignment of Homologous sequences identified from a BLASTP[4] search of a nonredundant protein database. The query sequence was the C-terminal 14 amino acids from human platelet factor 4 (row 1). Results included Platelet factor 4 sequence from a diverse range of mammals. Conserved amino acids are shown in blue, divergent amino acids are unshaded.

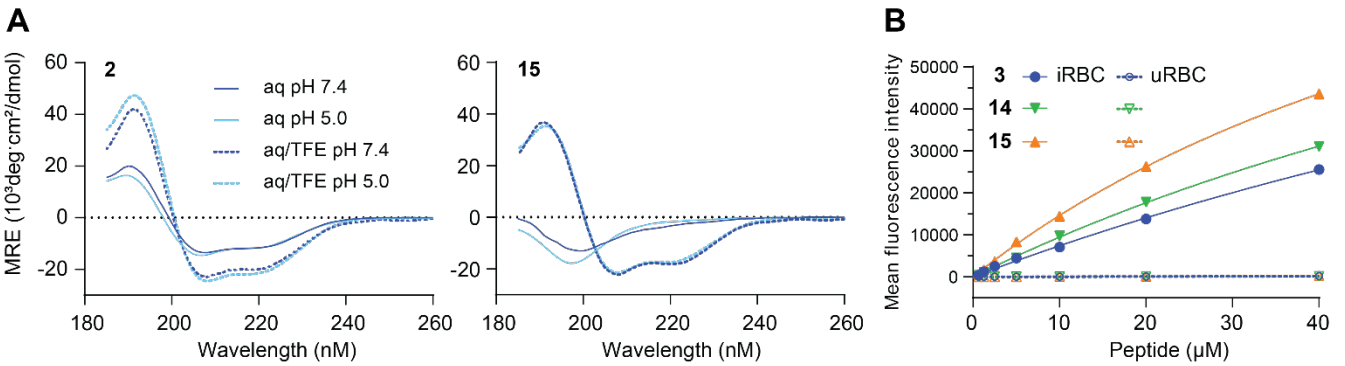

Figure S4. Comparative Structural and Cell Penetrating Characteristics of Analogues with Reduced Potency. Peptides: **2**, truncated scaffold; **3**, full length scaffold; **14**, Ile to Val substitution; **15**, Leu to His (2) and Ser to Arg (1) substitutions. (**A**) Spectra were collected for 50 μM peptides in aqueous solution (aq, 100 mM NaF, 10 mM KH_2PO_4) adjusted to either pH 7.4 or pH 5.0, and 50% aqueous solution with 50% trifluoroethanol (aq/TFE). Spectral minima at 218–222 nm indicates α-helical structure; (**B**) Selective entry of peptides labelled with AlexaFluor-488 into infected red blood cells (iRBC) compared to uninfected RBC (uRBC). Data represent mean fluorescence intensity for 100,000 events (flow cytometry) following treatment of RBC with increasing concentrations of labelled peptides for 1 h, from a single experiment.

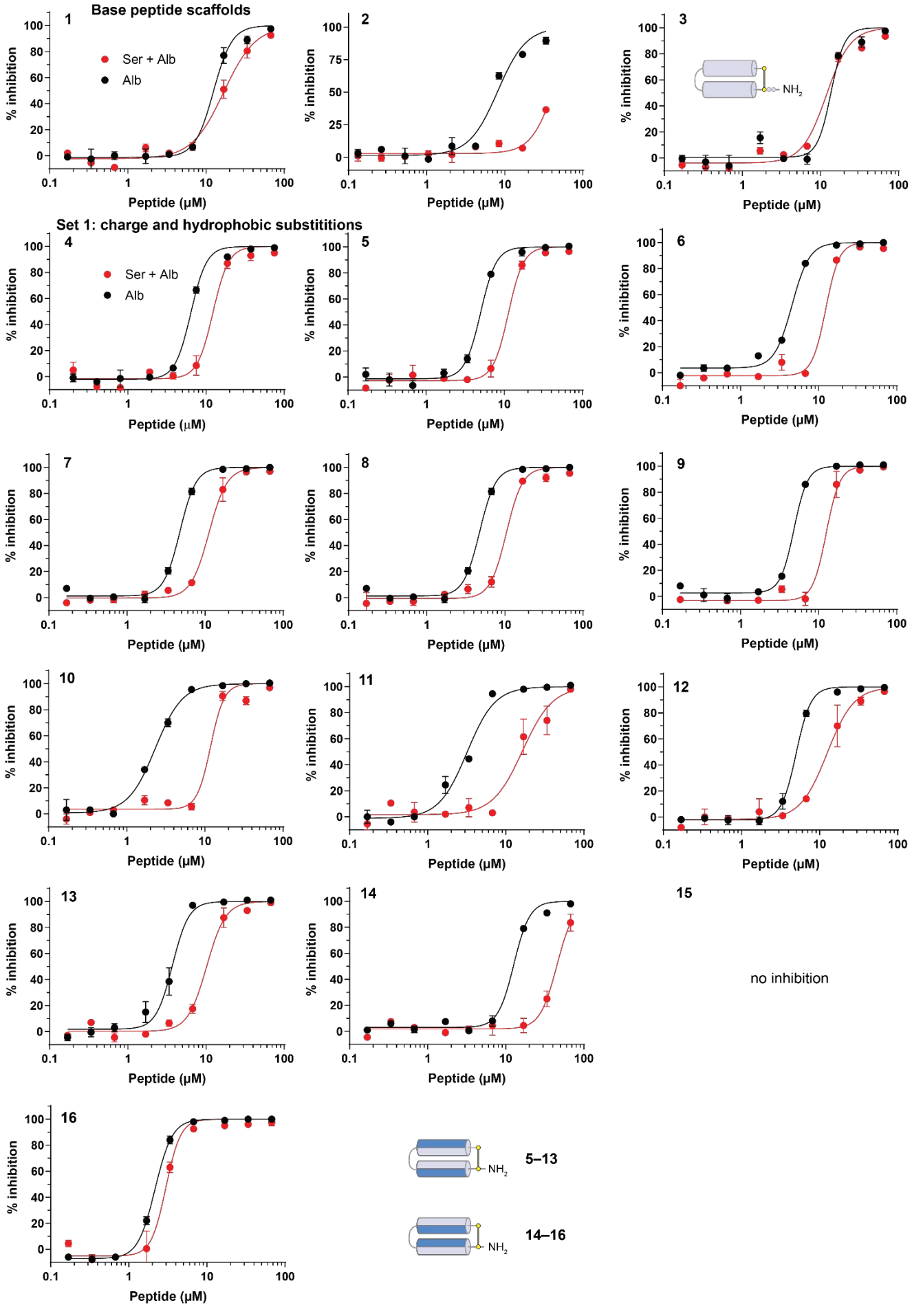
Base peptide scaffolds
1
Ser + Alb
Alb
% inhibition
Peptide (μM)
2
3
NH2
Set 1: charge and hydrophobic substitutions
4
5
6
7
8
9
10
11
12
13
14
15
no inhibition
16
5–13
14–16

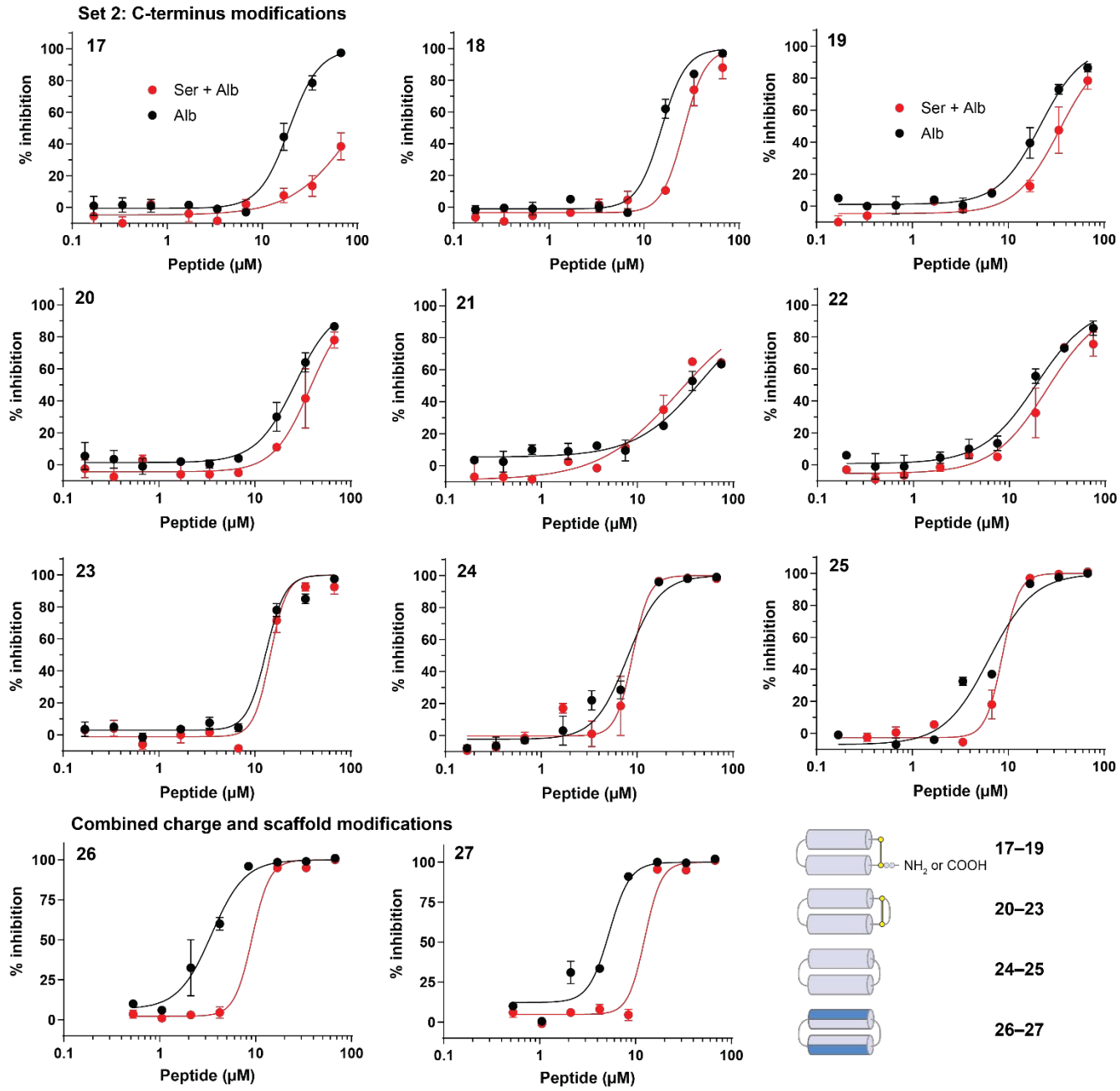

Figure S5. Dose Response Curves Showing *In Vitro* Growth Inhibition of *Plasmodium falciparum* 3D7 Parasites Treated with Serially Diluted Peptides. RPMI culture media was either supplemented with 5% human serum, 2.5 mg/mL Albumax II, Ser + Alb (red); or 5 mg/mL Albumax II, Alb (black). Parasites were incubated with serially diluted peptides in supplemented culture media for 72 h at 37 °C, 5% CO_2 and 5% O_2. Growth inhibition was examined using a high throughput microscopic assay where parasite counts were determined from DAPI-stained nuclei.[5] Data points represent two independent experiments with standard error. Curves were fitted using GraphPad Prism v 10.0.2 [inhibitor] versus response with four parameters and constraining the top of the curve to 100%. IC_{50} values determined from the curves are shown in Table 1.

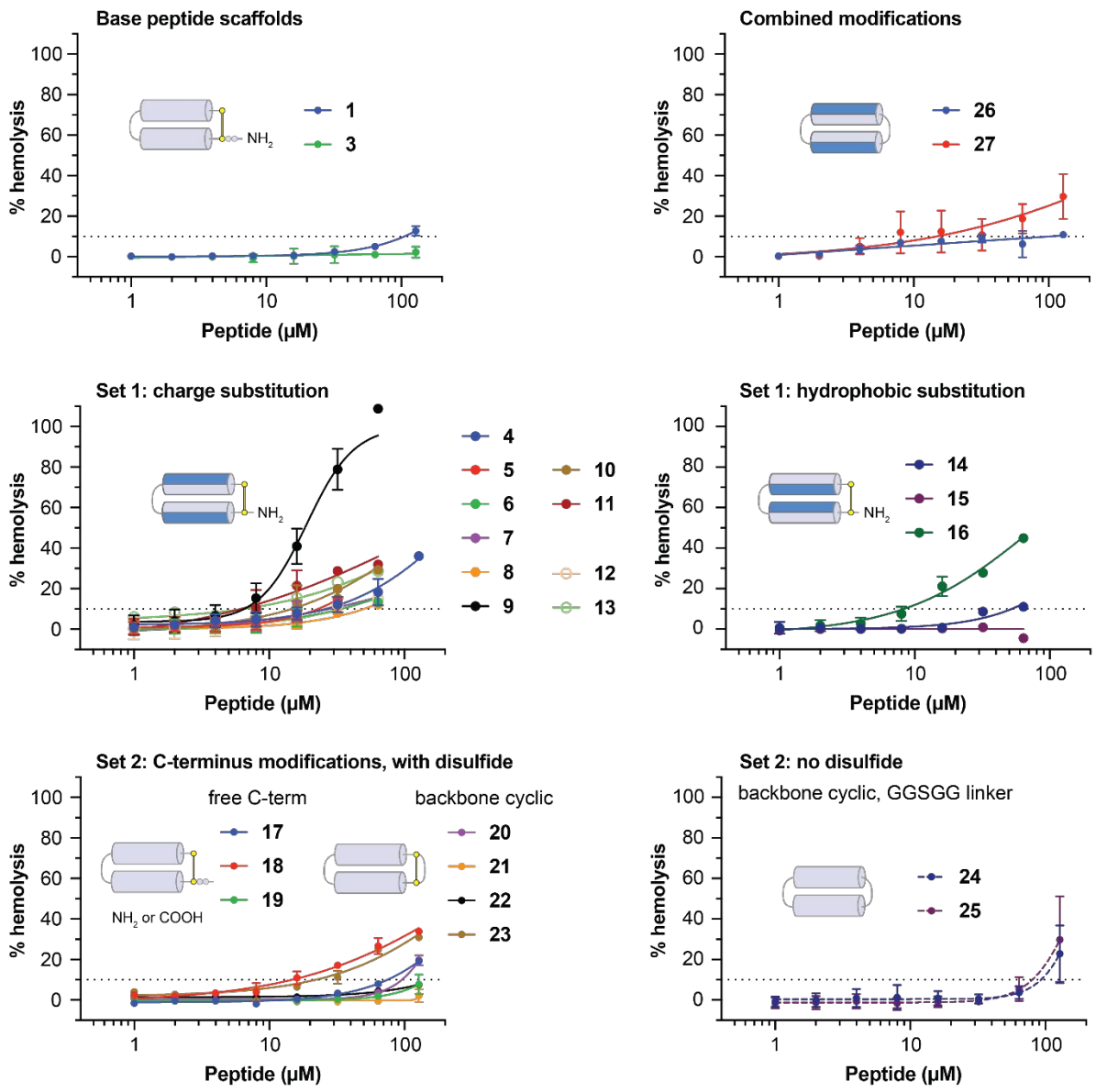

Figure S6. Dose Response Curves Showing Hemolysis of Human RBCs Treated with Serially Diluted Peptides. RBCs at 0.25% hematocrit in phosphate buffered saline (PBS) were incubated with peptides for 1 h at 37 °C. RBC hemolysis was determined by measuring hemoglobin released into the culture supernatant compared to 0% (no treatment) and 100% (0.1% Triton-X 100) controls. Data represent the mean and standard error from two biological replicates. The minimal hemolytic concentration required to lyse 10% of RBCs (HC_{10}) was determined from the dose-response curves using Graphpad Prism v 10.0.2. HC_{10} values are summarized in Table 1.

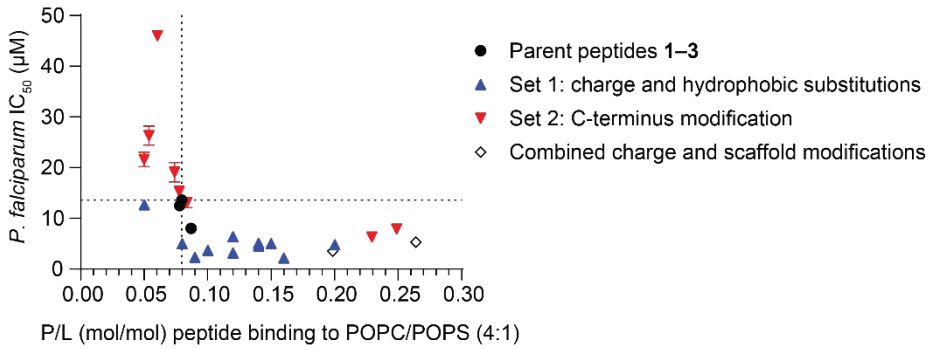

Figure S7. Relationship Between PDIP Analogues Binding to POPC/POPS (4:1) Bilayers and *In Vitro* Activity Against *P. falciparum*. P/L ($RU_{peptide}/mw_{peptide}$)/($RU_{lipid}/mw_{lipid}$) was determined from the end of the association phase (170 s) of SPR sensorgrams, for 16 μM PDIP analogues binding to POPC/POPS (4:1) bilayers; *P. falciparum* IC_{50} values were determined from *in vitro* cultures of *P. falciparum* 3D7 assayed in RPMI culture media supplemented with 5 mg/mL Albumax II (serum free condition). Reference lines are shown for parent peptide **3**.

REFERENCES

(1) Lawrence, N.; Dennis, A. S. M.; Lehane, A. M.; Ehmann, A.; Harvey, P. J.; Benfield, A. H.; Cheneval, O.; Henriques, S. T.; Craik, D. J.; McMorran, B. J. Defense peptides engineered from human platelet factor 4 kill *Plasmodium* by selective membrane disruption. *Cell Chem. Biol.* **2018**, *25* (9), 1140-1150.

(2) Lawrence, N.; Philippe, G. J. B.; Harvey, P. J.; Condon, N. D.; Benfield, A. H.; Cheneval, O.; Craik, D. J.; Troeira Henriques, S. Cyclic peptide scaffold with ability to stabilize and deliver a helical cell-impermeable cargo across membranes of cultured cancer cells. *RSC Chem. Biol.* **2020**, *1* (5), 405-420.

(3) Palombi, I. R.; Lawrence, N.; White, A. M.; Gare, C. L.; Craik, D. J.; McMorran, B. J.; Malins, L. R. Development of antiplasmodial peptide–drug conjugates using a human protein-derived cell-penetrating peptide with selectivity for infected cells. *Bioconjug. Chem.* **2023**, *34* (6), 1105-1113.

(4) Johnson, M.; Zaretskaya, I.; Raytselis, Y.; Merezhuk, Y.; McGinnis, S.; Madden, T. L. NCBI BLAST: a better web interface. *Nucleic Acids Res.* **2008**, *36* (Web Server issue), W5-9.

(5) Duffy, S.; Avery, V. M. Development and optimization of a novel 384-well anti-malarial imaging assay validated for high-throughput screening. *Am. J. Trop. Med. Hyg.* **2012**, *86* (1), 84-92.